

# Detection of paramagnetic recombination centers on the surface of silicon wafers

© L.S. Vlasenko

Ioffe Institute,  
194021 St. Petersburg, Russia  
E-mail: Leovlas@solid.ioffe.ru

Received May 20, 2024

Revised June 20, 2024

Accepted July 5, 2024

The electron paramagnetic resonance spectra of centers localized on the (111), (110), and (100) oriented surfaces of silicon wafers were observed and investigated using the spin dependent recombination change in microwave photoconductivity of samples. It was shown that dominant recombination centers created after natural oxidization on air at room temperature on the (111)- and (110)-surfaces are the silicon dangling bond centers, so called Pb-centers. On (100)-surface the pairs of dangling bonds are responsible for spin dependent recombination. The optimal experimental conditions such as microwave power, light intensity, and temperature were discussed for detection of surface recombination centers with higher sensitivity compared to usual electron paramagnetic resonance method.

**Keywords:** silicon, surface, spin dependent recombination, electron paramagnetic resonance.

DOI: 10.61011/SC.2024.05.59173.6715

## 1. Introduction

The centers on the surface of silicon crystals and at Si/SiO<sub>2</sub> interface influence the recombination processes of non-equilibrium carriers, characteristics of various semiconductors and their degradation processes [1–4]. The surface centers in silicon have been extensively studied for over several decades. The main method of studying such centers is the method of electron paramagnetic resonance (EPR), which allows not only identifying their microstructure, but also studying the behavior of the centers under various surface treatments [5–9]. However, the EPR method requires a fairly high surface density of paramagnetic centers (of the order  $10^{12}$ – $10^{13}$  cm<sup>-2</sup>), which is achieved in case of high-temperature (800–1200°C) oxidation of the silicon surface [9]. In such samples the centers' EPR spectra with a spin  $S = 1/2$ , the so-called P<sub>b</sub>-centers on (111) and (110) surfaces and centers P<sub>b0</sub> and P<sub>b1</sub> on (100) surface were discovered and studied in details. To increase the EPR spectra intensity and for better signal-to-noise ratio the samples composed of 10–20 thin silicon wafers < 80 μm thick are usually used, as well as the accumulation of spectra during repeated magnetic resonance passage [8,9].

Of high interest is the development of relatively simple methods of detection and study of a microstructure and properties of the surface centers originating from natural oxidation, as well as from different treatment methods of silicon wafers used in today's electronics. A significant (by several orders of magnitude) increase of EPR method sensitivity was demonstrated in previous studies using methods for EPR spectra registration by resonant changes in the microwave photoconductivity of crystals [10–12] using spin-dependent recombination (SDR) effects. Photoconductivity variations may be registered from both, the

change in the photocurrent passing through the sample and the change of the microwave photoconductivity due to absorption of electrical component of the microwave field in EPR resonant cavity of the spectrometer. The free path of photo-excited carriers is comparable to the thickness of thin, 100–300 μm wafers of pure high-resistance silicon, and their recombination is determined mainly by surface centers. A change of the spin state of these centers during magnetic resonance shortens the lifetime of nonequilibrium carriers, which results in a decrease of photoconductivity in the crystal volume. This effect served the basis for the earlier conducted experiments for registration and study of SDR-EPR spectra of recombination centers in thin near-surface silicon layers impregnated with ions of hydrogen [13], arsenic [14], bismuth [15], and also new recombination centers in the form of dangling bonds pairs [16] were discovered on the (100) oriented silicon wafers surface.

Currently, the methods of electrical detection of magnetic resonance (EDMR) in semiconductor MDT structures with the use of electrical contacts for registration of the spin-dependent current variation through Si/SiO<sub>2</sub> structures [17,18] and silicon carbide structures [19] are being extensively developed. Based on SDR and EDMR effects in SiC structures the semiconductor sensors of magnetometers were designed [20,21]. Additionally, the studies of Si/SiC structures [22], including SDR studies in such structures are in progress [23].

This paper outlines the findings of studies of EPR spectra basic registration patterns for paramagnetic recombination centers on the surface of silicon wafers and in Si/SiO<sub>2</sub> layers without the use of electrical contacts. Due to the method of detecting the microwave photoconductivity variations under magnetic resonance it became possible to study

the EPR spectra in silicon crystals specifically subjected to the high-temperature oxidation, while in case of using conventional EPR method no any spectra can be observed. The best experimental conditions for detecting the surface paramagnetic recombination centers were analyzed. It was shown that the spin-dependent recombination centers on the silicon surfaces (111) and (110) differ from the centers on (100) surfaces in both, the symmetry and the response to chemical treatment with hydrofluoric acid.

## 2. Experimental procedure

The experiments were carried out with the silicon samples cut out from commercial silicon wafers of *n*-type having (111), (110), (100) surface orientations and resistivity of  $\rho = 0.1\text{--}3\text{ k}\Omega\cdot\text{cm}$  and thickness of  $h = 0.25\text{--}0.3\text{ mm}$ .

The SDR-EPR spectra were recorded using EPR spectrometer with a three-centimeter range with a maximum microwave field power of 80 mW. Samples with a size of  $3.5 \times 8 \times h\text{ mm}$  with a long edge directed along the axis of the crystal of  $\langle 110 \rangle$  were placed along the axis of the cylindrical resonator into the antinode of the magnetic component of the microwave field  $H_1$  perpendicular to the constant magnetic field  $B$ . The photoconductivity was excited by the light of 100 W incandescent lamp. The absorption of the electrical component  $E_1$  by free carriers was also observed at the same time, which manifested itself in a decrease of the Q-factor of the resonator when the light was turned on. SDR-EPR signals were registered based on the change in resonator Q factor during scanning of magnetic field  $B$ , similar to the registration of conventional EPR signals using magnetic field modulations  $B$  at 100 kHz and synchronous detecting for registration of the first absorption signal derivative with respect to magnetic field. However, when detecting the microwave photoconductivity with respect to absorption of  $E_1$  component it is required to allow for the quite long lifetimes of the non-equilibrium carriers that, in pure silicon crystals, are longer than modulation period of magnetic field equal to  $10^{-5}\text{ s}$ , which requires a phase shift of the synchronous detector.

To provide better resolution of lines in SDR-EPR spectra their detecting was carried out as a second absorption derivative with respect to 100 kHz and 100 Hz magnetic field modulations and 0.1 and 0.05 mT modulation amplitudes, respectively, with alternating synchronous detecting at these frequencies.

To identify the SDR-EPR spectra the angular dependencies of EPR lines position during the sample rotation around the axis of  $\langle 110 \rangle$  crystal were studied and results were compared with the literature data. Magnetic field was calibrated along the lines of EPR ions  $\text{Mn}^{2+}$  in MgO powder in the quartz tube located near the studied silicon sample at room temperature. Measurements were generally made at temperature of liquid nitrogen. The temperature dependencies of the surface recombination centers' SDR-EPR spectra, in particular with the silicon

wafers with a resistivity of  $5\text{ }\Omega\cdot\text{cm}$ , were studied at temperatures 10–300 K with the use of helium continuous-flow cryostat.

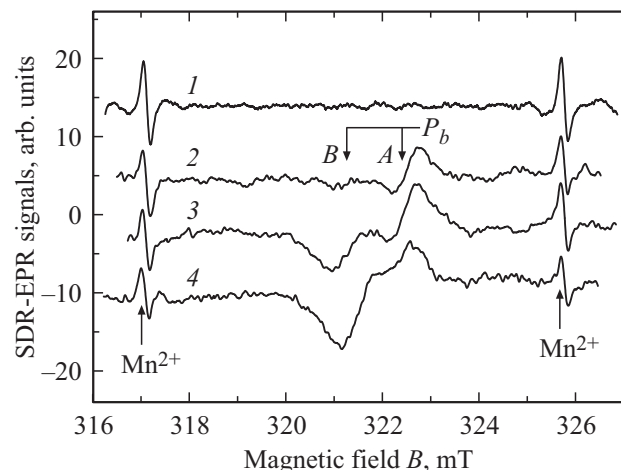
To study the impact of oxide layer on SDR-EPR spectra the surface was treated with a 50% aqueous solution of HF for 1–5 minutes and the spectra were being registered for several weeks with natural oxidation of silicon in the air at room temperature.

## 3. Results and discussion

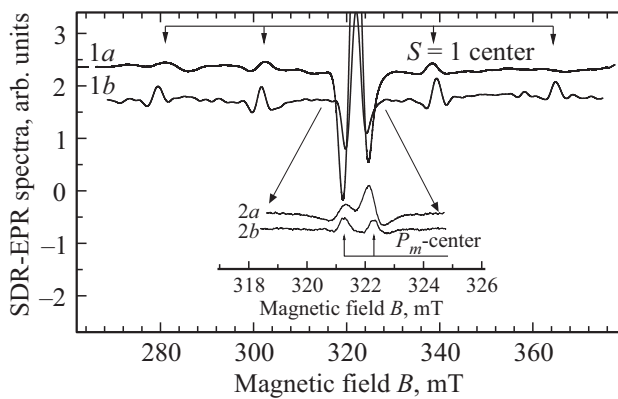
### 3.1. SDR-EPR spectra of recombination centers

Figure 1 shows the spectra of paramagnetic resonance registered at room temperature in the samples cut out from the high-resistance ( $\rho > 1000\text{ }\Omega\cdot\text{cm}$ ) silicon wafers with (111), (110) and (100) surface orientations, as well as the third and fourth of six EPR lines of the ultra-fine  $\text{Mn}^{2+}$  ions structure in the calibration sample. Without lighting no EPR spectra are observed (Figure 1, spectrum 1).

In presence of light the spectra (Figure 1, spectra 2–4) occur the lines of which have a sign opposite to the standard EPR lines from the manganese ions and indicating the increase of EPR spectrometer resonant cavity Q factor under magnetic resonance. This indicates that in magnetic resonance of the surface centers the rate of light-excited carriers recombination increases, their concentration goes down, as well as absorption of  $E_1$  electrical component of the microwave field. Since the EPR spectra of the surface recombination centers can be observed already at room temperature on one sample, it indicates high sensitivity of the microwave photoconductivity at least



**Figure 1.** Paramagnetic resonance spectra of the recombination centers on the surfaces of silicon wafers without lighting (spectrum 1) and with lighting of high-resistance silicon wafers of *n*-type with the following surface orientations (111) — spectrum 2, (110) — spectrum 3 and (100) — spectrum 4. The spectra are written as a first absorption derivative with respect to the magnetic field at room temperature,  $B \parallel \langle 110 \rangle$  orientation of magnetic field and 9.0325 GHz. frequency of the microwave field.



**Figure 2.** SDR-EPR spectra of exited triplet state with  $S = 1$  spin (spectra *1a* and *1b*) and centers with  $S = 1/2$  spin (spectra *2a* and *2b*) of paramagnetic recombination centers on (100) surface of silicon of  $n$ -type having resistivity of  $2700 \text{ Ohm} \cdot \text{cm}$ . The spectra are written as a second absorption derivative with respect to the magnetic field at  $T = 77 \text{ K}$  and  $B \parallel (110)$  orientation of magnetic field. Spectra *1a* and *2a* — are given for initial sample, and spectra *1b* and *2b* — after surface etching with HF.

10 times higher compared to conventional EPR method where 10–20 silicon wafers packages are used for the studies.

At a temperature of liquid nitrogen the amplitude of SDR-EPR spectra of the surface recombination centers rises by an order which allows studying the surface centers behavior in a more detailed way in conditions of varying light intensity, microwave field power and temperature. Additionally, it becomes possible to register the spectra as a second absorption derivative with respect to magnetic field, thus, improving the lines resolution in the spectra and more precisely analyzing the lines positions angular dependencies, defining the spin parameters and symmetry of the paramagnetic recombination centers. In previous paper [24] it was shown that the main spin-dependent recombination centers on (111) and (110) surfaces are  $P_b$ -centers featuring a trigonal ( $C_{3v}$ ) symmetry of  $g$ -tensor along the axis of  $\langle 111 \rangle$  crystal with its principal values of  $g_{\parallel} = 2.00136$  and  $g_{\perp} = 2.0088$ . On (111) surface  $P_b$ -centers are oriented mainly perpendicular to the surface on the surface, which corresponds to the most intense line *A* as shown in Figure 1 (spectrum 2). On (110) surface  $P_b$ -centers are oriented in two directions  $\langle 111 \rangle$  in (110) plane perpendicular to the surface. This results in the appearance of two lines (*A* and *B*) in SDR-EPR spectrum (see Figure 1, spectrum 3).

The main recombination centers on (100)-surface of silicon are  $P_m$ -centers [16], which are the pairs of dangling bonds of adjacent silicon atoms oriented along two mutually perpendicular directions  $\langle 110 \rangle$  on this surface. Similar to *A*-center in the irradiated silicon (a complex of oxygen+vacancy) [25,26] the adjacent dangling bonds of silicon atoms form binding and anti-binding orbitals. Two electrons with anti-parallel spins are localized on

the binding orbital. When the photoexcited electron is captured in the anti-binding orbital (or capturing of hole in the binding orbital) the center will be paramagnetic with the spin  $S = 1/2$ .  $P_m$ -centers have  $S = 1/2$  spin and an orthorhombic symmetry ( $C_{2v}$ ) of  $g$ -tensor with the main values of components  $g_1 = 2.0093$ ,  $g_2 = 2.0029$  and  $g_3 = 2.0036$  [16].

During lighting as a result of sequential capture of the electron and hole  $P_m$ -center may be in the metastable excited state with a spin  $S = 1$ , when two electrons with parallel spins are located in different molecular orbitals: the binding and anti-binding ones. The SDR-EPR spectra of the excited triplet state of  $P_m$ -center on (100)-surface of silicon are shown in Figure 2.

Spectra *2a* and *2b* in Figure 2 are obtained with the lowest modulation amplitude and the best resolution of lines SDR-EPR are observed at  $B \cong 320 \text{ mT}$ . As seen in Figure 2, after surface treatment with HF the lines in the spectrum of triplet centers are narrowed, their amplitude is increased and distance between them becomes larger. Also, the change of the centers spectra lines with spin  $S = 1/2$  is observed. The impact of the oxide layer removal by etching in HF will be discussed further in sect. 3.4.

### 3.2. Specifics of SDR-EPR spectra detecting

The method of magnetic resonance spectra registration based on the change of samples microwave photoconductivity is applicable at sufficient sensitivity of EPR resonant cavity  $Q$  factor to the changes in photoconductivity when the light is activated. In experiments the samples were placed along the axis of cylindrical resonant cavity into the antinode of magnetic component  $H_1$  of the microwave field which induces the magnetic spin transitions of paramagnetic recombination centers. Because of limited dimensions of the samples and their slight offset from the resonant cavity's center, the electrical component  $E_1$  is also present in the bulk samples, and when carriers appear with activation of light it results in absorption of the microwave field.

Thus, SDR-EPR signals magnitude will be proportionate to the power of the microwave field  $P_{mw} \propto (H_1 E_1)$ , in contrast to conventional EPR signals when their magnitude is proportionate to  $(P_{mw})^{1/2} \propto H_1$ . Figure 3 illustrates the SDR-EPR signals amplitude of  $P_b$ -centers on surface Si(111) and amplitude of conventional EPR signals  $\text{Mn}^{2+}$  versus  $(P_{mw})^{1/2}$ .

Similar dependencies of SDR-EPR signals were observed for centers on (110) and (100) surfaces. Different behavior of conventional EPR and SDR-EPR signals indicates that when the spectra of surface paramagnetic centers are registered with the use of spin-dependent recombination effects both components of the microwave field — magnetic and electric — are included.

With the change of light intensity also the contribution of electrical component of the microwave field is manifested. Figure 4 shows the dependencies of the surface recombination centers signals amplitudes and amplitudes of EPR

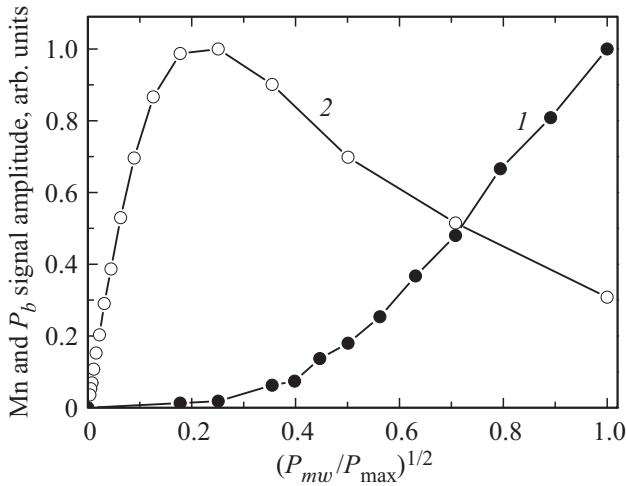


**Figure 3.** Amplitude of SDR-EPR signals of  $P_b$ -centers on Si(111) surface (curve 1) and amplitude of standard EPR signals  $Mn^{2+}$  (curve 2) versus  $(P_{mw}/P_{max})^{1/2}$ .

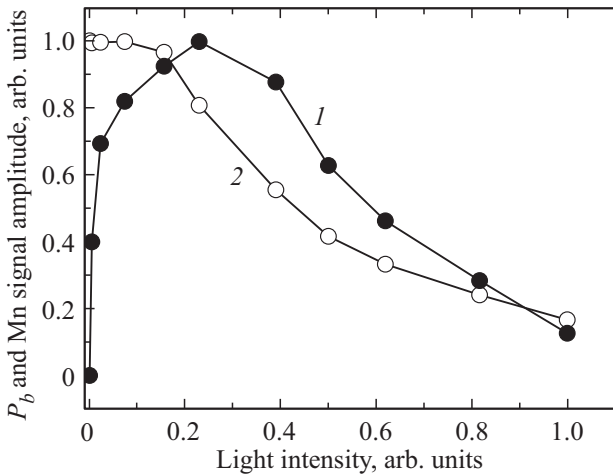


**Figure 4.** Amplitude of SDR-EPR signals of  $P_b$ -centers (curve 1) and EPR signals  $Mn^{2+}$  (curve 2) versus light intensity.

signals  $Mn^{2+}$  in MgO calibration sample with manganese impurity from the light intensity.

We see that SDR-EPR signals of  $P_b$ -centers (Figure 4, curve 1) increase with the growth of light intensity, reach their maximum and go down with further light intensity growth, with simultaneous decrease of signals from  $Mn^{2+}$  ions (Figure 4, curve 2). This decrease is related to the growth of stationary concentration of the photo-excited carriers, growth of absorption of  $E_1$  component and reduction of the resonant cavity's Q factor and lower sensitivity of EPR spectrometer.

The concentration of the photo-excited carriers at maximal light intensity can be evaluated by comparing the decrease in EPR spectrometer sensitivity by placing the non-illuminated silicon sample with lower resistivity into the resonant cavity. Similar decrease of amplitude of the calibration EPR signals of  $Mn^{2+}$  ions as with maximal light

intensity in Figure 4 was observed when placing into the resonant cavity the silicon sample of  $n$ -type with resistivity of 20–30  $\Omega \cdot \text{cm}$ , which corresponds to the concentration of electrons in the conduction band at room temperature  $\cong 2 \cdot 10^{14} \text{ cm}^{-3}$ . Thus, we may make a conclusion that when the high-resistance silicon is illuminated, then, practically the same concentration of the photo-excited carriers is observed.

According to the experiments, the paramagnetic recombination centers on the surface of silicon wafers within the temperature range 77–300 K may be carried out for samples with resistivity of  $> 100 \Omega \cdot \text{cm}$ . For samples with lower resistivity it is necessary to use lower temperatures.

### 3.3. Effect of temperature on SDR-EPR spectra

Figure 5 shows dependencies of amplitude of SDR-EPR spectra of  $P_b$ -centers on the silicon wafers surface of  $n$ -type having resistivity of 5 and 2500  $\Omega \cdot \text{cm}$ .

As seen from Figure 5 (curve 1), the EPR spectra of the spin-dependent recombination surface centers in silicon with low resistivity are observed at temperatures below 40 K, when the conductivity electrons are localized at the levels of phosphorous donor impurity. At these temperatures the concentration of the photo-excited electrons significantly outpaces their equilibrium concentration. In high resistivity silicon the SDR-EPR spectra of surface centers are observed up to the room temperature (see Figure 5 curves 2–4).

Presumably, the increase of SDR-EPR spectra of surface centers with the decrease of temperature from 300 to 70 K is related with the increase of spin polarization degree of paramagnetic centers  $P_s \propto \exp(\mu B/kT)$ . Here

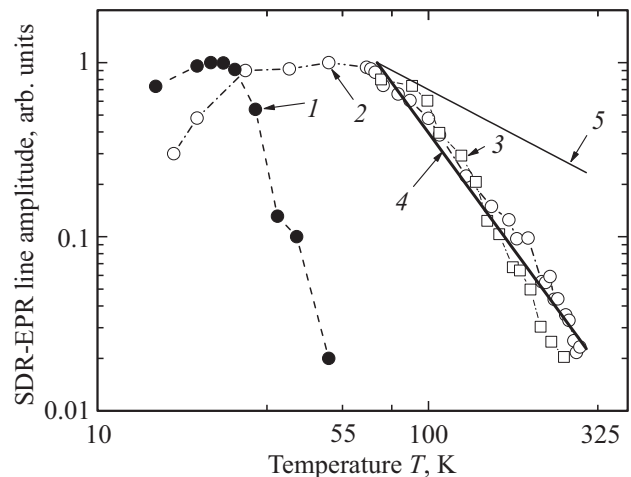


**Figure 5.** Experimental curves of the surface centers SDR-EPR spectra amplitude versus temperature for samples  $n$ -Si 5  $\Omega \cdot \text{cm}$  with (111) surface orientation — curve 1,  $n$ -Si 2500  $\Omega \cdot \text{cm}$  with (111) surface orientations — curve 2 and (100) — curve 3. Line 4 — calculated dependence  $T^{-2.6}$ , proportionate to the temperature dependence of electrons mobility in the high-resistance silicon [27]. Line 5 — dependence  $T^{-1}$ , corresponding to behavior of Boltzmann spin polarization.

$\mu$  — magnetic moment of electron,  $k$  — Boltzmann constant. At  $B = 0.325$  mT and temperature  $> 77$  K the value  $\mu B/kT \ll 1$  and ratio of signals magnitude versus temperature shall be proportionate to  $T^{-1}$  (see. Figure 5, line 5) and shall grow with the temperature decrease below 77 K. However, as seen from the experimental data, the magnitude of SDR-EPR spectra rises faster than ( $T^{-1}$ ) at the temperature decrease from 300 to 77 K and goes down at the temperatures below 25 K. Such behavior is peculiar to the temperature dependence of the electrons mobility, which in the temperature range of 300–77 K is defined by the scattering on phonons and depends from the temperature as  $T^{-\alpha}$  at  $\alpha = 1.5$ .

For silicon, the power exponent is generally higher  $\alpha = 2.4–2.6$  [27]. The dependence proportionate to  $T^{-2.6}$  is shown in Figure 5 (line 4). Thus, from the analysis it follows that the magnitude of the surface centers EPR signals registered using the spin-dependent microwave photoconductivity is not influenced by the centers' spin polarization but is defined by the mobility of the photoexcited electrons.

### 3.4. Oxide layer effect on the SDR-EPR spectra of surface centers

The studied paramagnetic centers are localized at Si/SiO<sub>2</sub> interface. The oxide layer on silicon always appears during storage at room temperature and may reach dozens of angstroms [28]. Chemical etching of silicon surface in hydrofluoric acid results in removal of SiO<sub>2</sub> and change of SDR-EPR spectra of the surface centers.

$P_b$  centers are not observed right after treatment of surfaces (111) and (110) with HF, which is because of passivation of silicon dangling bonds with hydrogen atoms [8]. However, the spectra of these centers appear with time when the samples are stored in the air at room temperature and reach their initial level in two-three weeks. This is shown in Figure 6.

Other type of SDR-EPR spectra behavior is observed when treating the (100) orientation surface. On this surface, the EPR spectra of centers with  $S = 1/2$  spin were found and studied, e.g.  $P_{b0}$  and  $P_{b1}$  associated with single dangling bonds of silicon atoms at Si/SiO<sub>2</sub> interface [5]. These centers have component values of  $g$ -tensor, close to the values of  $P_b$ -centers, and their SDR-EPR lines have insufficient resolution and may be overlapped by the lines of  $P_m$ -centers [16], leading to wider lines of the spectrum shown in Figure 2 (spectrum 2a). After treatment of (100) surface with HF the intensity of SDR-EPR spectrum lines is reduced and the two lines corresponding to  $P_m$ -centers (see Figure 2, spectrum 2b) are clearly observed. Passivation of single dangling bonds of  $P_{b0}$ - and  $P_{b1}$ -centers probably occurs here, similar to  $P_b$ -centers. Apparently, the capture of hydrogen atoms by  $P_m$ -centers, which are themselves the pairs of nearest silicon dangling bonds, is less efficient.

As seen from Figure 2, the amplitude of SDR-EPR spectrum of the excited triplet state of  $P_m$ -center (spec-

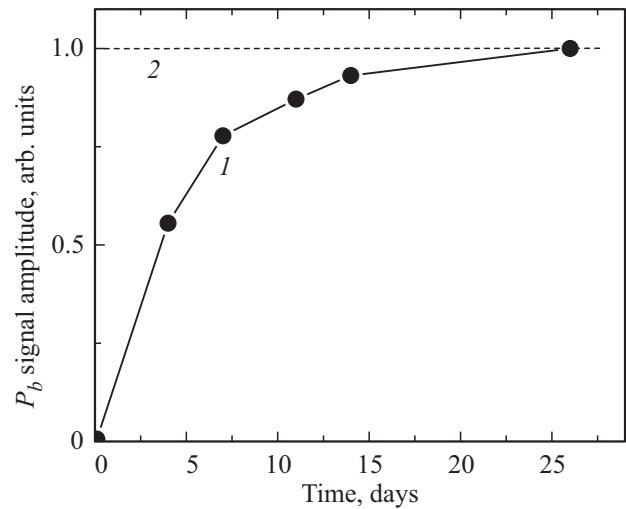


**Figure 6.** Amplitude of SDR-EPR signals of  $P_b$ -centers on Si(111) surface versus sample oxidation time in the air at room temperature after etching with HF for 5 min (curve 1). Signal level in the initial sample (curve 2).

trum 1b) is increased after removal of the oxide layer, its lines are narrowed and the distance between the lines of fine structure at  $B \cong 280$  and 364 mT is enlarged. For the centers with spin  $S = 1$  the splitting of the fine structure is defined by a dipole magnetic interaction between two electrons of adjacent dangling bonds of silicon atoms and depends on the distance  $r$  between them as  $1/r^3$  [29]. The oxide layer induced mechanical pressure, by increasing the distance  $r$ , leads to the decrease of dipole interaction and reduction of distance between the lines of SDR-EPR spectrum. Additionally, mechanical stress leads to wider lines in the spectrum. It should be noted that after removal of the oxide layer the spectra 1b and 2b, shown in Figure 2, return to the initial spectra 1a and 2a, as samples undergo natural oxidation with time in the air, in the way as  $P_b$ -centers appear as shown in Figure 6.

## 4. Conclusion

Thus, it was shown that the effects of the spin-dependent recombination and microwave photoconductivity detection allow registering and studying the paramagnetic centers on the surface of commercial silicon wafers in a wide range of temperatures with a sensitivity by an order of magnitude higher than with registration by conventional EPR method. The basic patterns and optimal experimental conditions for detecting EPR spectra of surface recombination centers have been found. It was shown that intensity of SDR-EPR spectra grows linearly with the increase of power of the microwave field  $P_{mw}$ , in contrast to conventional EPR signals, the magnitude of which is proportional to  $P_{mw}^{1/2}$  at low power levels and is reduced with further increase in  $P_{mw}$ . To register SDR-EPR spectra, it is necessary to select the optimal light intensity, at which the absorption

of the microwave field by photo-excited carriers does not significantly reduce the Q-factor of EPR spectrometer resonator cavity and its sensitivity.

It was demonstrated that the main centers participating in the processes of spin-dependent recombination on Si(111) and Si(110) surfaces are the dangling bonds of silicon atoms localized at Si/SiO<sub>2</sub> interface (P<sub>b</sub>-centers). The SDR-EPR spectra of these centers disappear right after removal of the oxide layer after etching in HF and are restored in 2–3 weeks after natural oxidation in air. On Si(100) surface the main recombination centers are P<sub>m</sub>-centers which themselves are the pairs of silicon atoms dangling bonds and excited triplet states of these centers. On (100) surface etched in HF these recombination centers do not disappear.

The above-mentioned results allow suggesting that detection of SDR-EPR spectra at Si/SiO<sub>2</sub> interface with the use of spin-dependent microwave photoconductivity may be applied in control and studies of recombination centers behavior during various stages of silicon wafers surface treatment when fabricating the semiconductor devices. The main areas of the method application include the study of recombination centers passivation conditions (dangling bonds of silicon atoms) in order to increase the lifetime of nonequilibrium carriers, which is important in design of the photosensitive photodetectors and radiation detectors. It is considered essential to study the recombination centers not only at Si/SiO<sub>2</sub> interface, but also at the interface of silicon with other dielectric materials, as well as to study SiC structures on silicon surface.

## Funding

The study has been performed under the state assignment No. 0040-2019-0005.

## Acknowledgments

The author thanks I.S. Fedosov for her help in conducting experiments.

## Conflict of interest

The author declares that there's no conflict of interest.

## References

- [1] P.M. Lenahan, M.A. Jupina. *Colloid. Surf.*, **45**, 191 (1990).
- [2] M. Lannoo. *Revue Phys. Appl.*, **25**, 887 (1990).
- [3] P.M. Lenahan, J.F. Conley, jr. *J. Vac. Sci. Technol. B*, **16** (4), 2134 (1998).
- [4] C.R. Helms, E.H. Poindexter. *Rep. Progr. Phys.*, **57**, 791 (1994).
- [5] E.H. Poindexter, P.J. Caplan, B.E. Deal, R.R. Razouk. *J. Appl. Phys.*, **52** (2), 879 (1981).
- [6] K.L. Brower. *Semicond. Sci. Technol.*, **4**, 970 (1989).
- [7] K.L. Brower. *Phys. Rev. B*, **33** (7), 4471 (1986).
- [8] K.L. Brower. *Phys. Rev. B*, **38** (14), 9657 (1988).
- [9] A. Stesmans, V.V. Afanas'ev. *J. Appl. Phys.*, **83** (5), 2449 (1998).
- [10] L.S. Vlasenko, M.P. Vlasenko, V.N. Lomasov, V.A. Khramtsov. *ZhETF* **91**, 1037 (1986). (in Russian).
- [11] L.S. Vlasenko. *FTT*, **41** (5), 774 (1999). (in Russian).
- [12] L.S. Vlasenko. *Appl. Magn. Reson.*, **47**, 813 (2016).
- [13] L.S. Vlasenko, M.P. Vlasenko, V.A. Kozlov, V.V. Kozlovskii. *FTP*, **33** (10), 1164 (1999). (in Russian).
- [14] D. P. Franke, M. Otsuka, T. Matsuoka, L. S. Vlasenko, M.P. Vlasenko, M.S. Brandt, K.M. Itoh. *Appl. Phys. Lett.*, **105**, 112111 (2014).
- [15] P.A. Mortemouque, T. Sekiguchi, C. Culan, M.P. Vlasenko, R.G. Elliman, L.S. Vlasenko, K.M. Itoh. *Appl. Phys. Lett.*, **101**, 082409 (2012).
- [16] H. Saito, S. Hayashi, Y. Kusano, K.M. Itoh, M.P. Vlasenko, L.S. Vlasenko. *J. Appl. Phys.*, **123**, 161582 (2018).
- [17] Elias B. Frantz, Nicholas J. Harmon, David J. Michalak, Eric M. Henry, Michael E. Flatté, Sean W. King, James S. Clarke, Patrick M. Lenahan. *J. Appl. Phys.*, **130**, 234401 (2021).
- [18] Kenneth J. Myers, Patrick M. Lenahan, James P. Ashton, Jason T. Ryan. *J. Appl. Phys.*, **132**, 115301 (2022).
- [19] C.J. Cochrane, P.M. Lenahan. *J. Appl. Phys.*, **112**, 123714 (2012).
- [20] Corey J. Cochrane, Jordana Blacksborg, Mark A. Anders, Patrick M. Lenahan. *Sci. Reports*, **6**, 37077 (2016).
- [21] Hesham Okeil, Gerhard Wachutka. *Appl. Phys. Lett.*, **124**, 192101 (2024).
- [22] S.A. Kukushkin, A.V. Osipov. *Kondensirovannye sredy i mezhfaznye granitsy*, **24** (4), 407 (2022). (in Russian).
- [23] M.A. Anders, P.M. Lenahan, C.J. Cochrane, Johan van Tol. *J. Appl. Phys.*, **124**, 215105 (2018).
- [24] L.S. Vlasenko, I.S. Fedosov. *Pis'ma ZhTF*, **50** (9), 3 (2024). (in Russian).
- [25] G. Bemski. *J. Appl. Phys.*, **30** (8), 1195 (1959).
- [26] K.L. Brower. *Phys. Rev. B*, **4** (6), 1968 (1971).
- [27] T.A. Pagava, N.I. Maisuradze, M.G. Beridze. *FTP*, **45** (5), 582 (2011). (in Russian).
- [28] M. Morita, T. Ohmi, E. Hasegawa, M. Kawakami, M. Ohwada. *J. Appl. Phys.*, **68** (3), 1272 (1990).
- [29] J. Vertz, J. Bolton. *Teoriya i prakticheskie prilozheniya metoda EPR* (M., Mir, 1975) ch. 10.

*Translated by T.Zorina*